Topologies of Three-Phase Rectifier with Near Sinusoidal Input Currents – A Comparative Analysis of Power Quality Indices using FFT and DWT

Constantin Filote*[1,2], Viorel Apetrei[1], Adrian Graur[1]
[1]*Electrical Engineering and Computer Science Faculty*
Stefan cel Mare University of Suceava
University Street no. 13, 720029 Suceava, Romania
[2]*GermaroElectronics SRL, Suceava, Romania*
Email: filote@eed.usv.ro , viorela@eed.usv.ro, and adrian.graur@usv.ro

***Abstract* - The traditional method used to detect and localize power quality disturbances by Fast Fourier Transform (FFT) can provide only amplitude - frequency information, but looses time information. In evaluating power supply quality, the FFT-based indices present different limitations. This paper proposes a set of four indices based on Discrete Wavelet Transform (DWT), such as total harmonic distortion, equivalent distortion index, K-factor, and crest factor that can be also applied for non-stationary signals analysis, in unbalanced three-phase systems with non-sinusoidal conditions. In the comparative analysis of Power Quality Indices (PQIs) definitions, these two instruments were used for the three-phase power systems with non-linear loads: three rectifier topologies with near sinusoidal input currents (RNSIC).**

Keywords—Discrete Wavelet Transform (DWT), data acquisition system, Power Quality Indices (PQIs), rectifier with near sinusoidal currents (RNSIC), harmonics.

I. Introduction

In recent years, electric power quality has been receiving great interest due to the increased usage of nonlinear loads in the power systems area [1-5].

The power systems can suffer from different waveform distortions caused by multiple power quality disturbances, which can be classified as stationary (with time unchangeable characteristics) or non-stationary (with time changeable characteristics), sinusoidal or non-sinusoidal, respectively [6-13], [33-35].

The Power Quality Indices (PQIs) evaluation based on the Fast Fourier Transform (FFT) involves limitations as high computational effort, time related information loss, and spectral leakage, therefore new approaches are necessary. Definitions that are more accurate can be obtained using Discrete Wavelet Transform (DWT), which provides representations for any non-stationary waveforms, preserves time-frequency information, and reduces the computational effort [14-17].

To reduce the current harmonics, many electric power applications use uncontrolled three-phase rectifiers with near sinusoidal input currents, called RNSICs, which offer high dynamic performances, and allow getting near sinusoidal input currents. Such a modern rectifier is the AC-to-DC converter, which comprises three input inductors, a three-phase bridge rectifier with diodes, and commutation capacitors that enhance the input currents and the power factors.

This paper proposes a comparative analysis of PQIs definitions based on Discrete Wavelet Transform (DWT), and on Fast Fourier Transform (FFT) based on IEEE Standard 1459-2010 [18, 19] for unbalanced nonlinear three-phase systems in sinusoidal regime using three rectifier topologies with near sinusoidal input currents (RNSIC). The generated waveforms are captured with a data acquisition system, which contains voltage and current Hall transducers.

II. The PQIs Definitions Based on FFT/DWT in the Three-Phase Systems Case

A precise detection and analysis of power quality information can be realized by applying the wavelet theory. The method presented in this study involves a layer-by-layer decomposition, choice of suitable sampling frequency and suitable mother wavelet, and a harmonic real-time tracking [12].

A. *IEEE Standard three-phase definitions*

In the case of non-sinusoidal regime, PQIs definitions can be deduced considering the balanced three-phase system as three single-phase systems [18, 19].

1. *Total Harmonic Distortion*

Based on the effective voltage and current, the equivalent total harmonic distortion can be calculated as follows:

$$\mathrm{THD}_{eV} = \frac{\mathrm{V}_{eH}}{\mathrm{V}_{e1}} \quad (1)$$

$$V_{eH} = \sqrt{\frac{V_{RSH}^2 + V_{STH}^2 + V_{TRH}^2}{9}}, \mathrm{V}_{e1} = \sqrt{\frac{\mathrm{V}_{RS1}^2 + \mathrm{V}_{ST1}^2 + \mathrm{V}_{TR1}^2}{9}}. \quad (2)$$

where V_{RS}, V_{ST} and V_{TR} are the line-to-line voltage for phases *R*, *S* and *T*, while the subscripts *1* and *H* represent the fundamental component and the non-fundamental harmonic components, respectively [20, 21].

The equivalent total harmonic distortion in the current case is defined as:

$$\mathrm{THD}_{e1} = \frac{\mathrm{I}_{eH}}{\mathrm{I}_{e1}} \quad (3)$$

978-1-4799-2060-0/14/$31.00 ©2014 IEEE

$$I_{eH} = \sqrt{\frac{I_{RH}^2 + I_{SH}^2 + I_{TH}^2}{3}}, \quad \mathrm{I_{e1}} = \sqrt{\frac{\mathrm{I_{R1}^2 + I_{S1}^2 + I_{T1}^2}}{3}}. \tag{4}$$

where I_R, I_S and I_T are the line currents for phases R, S and T [20].

2. Equivalent Distortion Index

When the fundamental component does not exist, it can be used the equivalent distortion index calculated as:

$$\mathrm{DIN_{eV}} = \frac{\mathrm{V_{eH}}}{\mathrm{V_e}}, \ \mathrm{DIN_{e1}} = \frac{\mathrm{I_{eH}}}{\mathrm{I_e}} \tag{5}$$

$$\mathrm{V_e} = \sqrt{\frac{\mathrm{V_{RS}^2 + V_{ST}^2 + V_{TR}^2}}{9}}, \ \mathrm{I_e} = \sqrt{\frac{\mathrm{I_R^2 + I_S^2 + I_T^2}}{3}}. \tag{6}$$

3. Transformer K-Factor

For each current phase, K-factor can be defined as a summation of harmonic currents generated by the non-linear load using the following algorithm:

$$\mathrm{I_{Rhar}^2} = \sum_{h=1}^{\infty} h^2 \mathrm{I_{Rh}^2}, \ \mathrm{I_{Shar}^2} = \sum_{h=1}^{\infty} h^2 \mathrm{I_{Sh}^2}, \ \mathrm{I_{Thar}^2} = \sum_{h=1}^{\infty} h^2 \mathrm{I_{Th}^2}. \tag{7}$$

The equivalent harmonic is represented by:

$$\mathrm{I_{ehar}} = \sqrt{\frac{\mathrm{I_{Rhar}^2 + I_{Shar}^2 + I_{Thar}^2}}{3}}. \tag{8}$$

Transformer K-factor can be calculated using relation (9):

$$\mathrm{K} = \frac{\mathrm{I_{ehar}}}{\mathrm{I_e}}. \tag{9}$$

4. Crest Factor

The crest factor that appears in three-phase system defines the impact on a waveform, and can be calculated as a ratio between the peak amplitude and RMS value of the current waveform:

$$\mathrm{CF_R} = \frac{\mathrm{I_{R\ peak}}}{\mathrm{I_{R\ rms}}}, \ \mathrm{CF_S} = \frac{\mathrm{I_{S\ peak}}}{\mathrm{I_{S\ rms}}}, \ \mathrm{CF_T} = \frac{\mathrm{I_{T\ peak}}}{\mathrm{I_{T\ rms}}}. \tag{10}$$

Generally, three-phase crest factor represents the maximum value identified on each phase:

$$\mathrm{CF_{ov}} = \max\{\mathrm{CF_R}, \mathrm{CR_S}, \mathrm{CF_T}\}. \tag{11}$$

B. Three-phase PQIs definitions based on DWT

1. Total Harmonic Distortion

In the time-frequency domain, THD can be defined as [22]:

$$\mathrm{THD_v^{DWT}} = \frac{\mathrm{V_{det}}}{\mathrm{V_{app}}} = \frac{\sqrt{\sum_{j\ge j_0} \mathrm{V_j^2}}}{\mathrm{V_{j_0}}}, \ \mathrm{THD_i^{DWT}} = \frac{\mathrm{I_{det}}}{\mathrm{I_{app}}} = \frac{\sqrt{\sum_{j\ge j_0} \mathrm{I_j^2}}}{\mathrm{I_{j_0}}}. \tag{12}$$

where $V_{j_0,x}$, $I_{j_0,x}$ represent the voltage and current RMS values of the lowest frequency band j_0, called approximated voltage (V_{xapp}) and approximated current (I_{xapp}) for any phase x of the three-phase, respectively. The sets of voltage and current RMS values $\{V_{j,x}\}$ and $\{I_{j,x}\}$ of each frequency band or wavelet-level higher than or equal to the scaling level j_0, are termed detailed voltage (V_{xdet}) and detailed current (I_{xdet}) for any phase x respectively [17, 20].

2. Equivalent Distortion Index

The voltage and current equivalent total harmonic distortion can be formulated as:

$$\mathrm{DIN_v^{DWT}} = \frac{\mathrm{V_{det}}}{\mathrm{V_e}} = \frac{\sqrt{\sum_{j\ge j_0} \mathrm{V_j^2}}}{\sqrt{\sum_j \mathrm{V_j^2}}}, \quad \mathrm{DIN_i^{DWT}} = \frac{\mathrm{I_{det}}}{\mathrm{I_e}} = \frac{\sqrt{\sum_{j\ge j_0} \mathrm{I_j^2}}}{\sqrt{\sum_j \mathrm{I_j^2}}}. \tag{13}$$

where V_e and I_e represent the effective RMS values for three-phase voltages and currents.

3. Transformer K-Factor

This factor can be computed starting from the harmonic weighted RMS phase currents for any phase x as:

$$\mathrm{I_{x\ lev}^2} = \sum_{n=1}^{2^j-1} \left(\mathrm{l_j^n}\right)^2 \left(\mathrm{I_{xj}^n}\right)^2 \tag{14}$$

where $\mathrm{l_j^n}$ is the center frequency of the sub-band of detail n and decomposition level j. The detail weighted effective RMS current, which can be defined as

$$\mathrm{I_{e\ lev}} = \sqrt{\frac{\mathrm{I_{R\ lev}^2 + I_{S\ lev}^2 + I_{T\ lev}^2}}{3}} \tag{15}$$

The K-factor is given by the ratio:

$$\mathrm{K^{DWT}} = \frac{\mathrm{I_{e\ lev}}}{\mathrm{I_e}}. \tag{16}$$

4. Crest Factor

The phase crest factor is calculated using the relation:

$$\mathrm{CF_x^{DWT}} = \frac{\max_k \{\mathrm{i_{k,x}}\}}{\mathrm{I_x}} \ \text{for } k = 0, 1, ..., 2^{N-j}-1 \tag{17}$$

where I_x is RMS current value. The phase crest factor indicates the impact of a waveform on each phase. For different values of j, different decomposition levels of the phase crest factors can be obtained.

The overall crest factor is computed as:

$$\mathrm{CF_{ov}^{DWT}} = \max_k \{\mathrm{CF_x^{DWT}}\} \ \text{for } x = \mathrm{R, S, T}. \tag{18}$$

III. The Rectifiers in Three-Phase Power Systems

In many power electronics applications for three-phase systems, with AC 50 or 60-Hz power supply, the alternative sinusoidal voltage must be converted in DC voltage. These applications are represented by the uninterruptible power supply from commutations (UPS systems), electrical drives with AC motors and static frequency convertors, which are using three-phase uncontrolled diode rectifiers [23-32].

A. The Rectifier with Near Sinusoidal Input Currents (RNSIC-1 topology)

The higher order harmonics deletion of the network current can be obtained not only by using the filtering systems (active or passive) or the PWM rectifiers, but also using a AC-DC converter, which has practically sinusoidal input current, also known as RNSIC (Rectifier with Near Sinusoidal Input Currents) [23-31].

This rectifier is a classic type of three-phase bridge rectifier with parallel diode capacitors and serial inductors attached. It can be seen in Figure 1.

The capacitors C_1-C_6 are DC capacitors with the same C value. The inductances L_R, L_S and L_T have the same L value, and are connected on AC side. To obtain near sinusoidal drawn phase-currents i_R, i_S, and i_T, the relation between the two values L and C has to be [30-31]:

$$0.05 \le LC\omega^2 \le 0.10 \tag{19}$$

The functioning principle of this rectifier can be explained using the following steps contained in a third period of the network frequency $T = 2\pi / \omega$ (ω is the angle frequency).

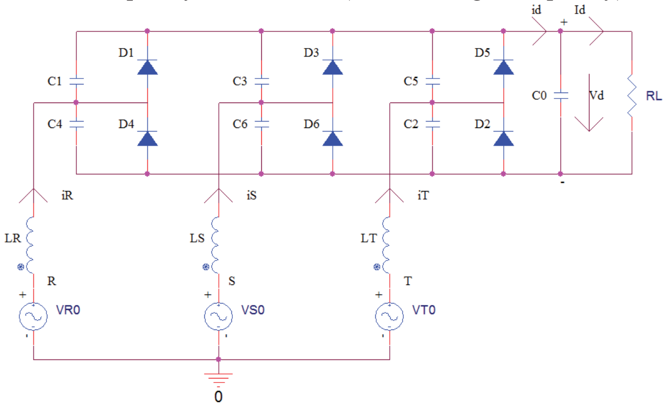

Figure 1. The RNSIC-1 electric scheme [23]

Two extreme situations of the RNSIC-1 convertor functioning can be discussed. In the first situation, if $R_L = 0$ (hence $V_d = 0$ and $\omega t_1 = 0$), the capacitors C_1-C_6 are short-circuited, and the angle $\varphi = +90^0$ is inductive. In this case, the phase currents are sinusoidal and have a I_{max} maximum amplitude [30].

In the second situation, if the V_d voltage is higher than $\sqrt{2}V_m/\left(1-2LC\omega^2\right)$ value, the diodes D_1-D_6 are no longer conductive and the $\varphi = -90^0$ angle is capacitive (hence $R_L = \infty$ and $\omega t_1 = \pi$). In this case, the phase currents i_R, i_S, and i_T are sinusoidal as well, and have a $\sqrt{2}\ I_{min}$ minimum value magnitude, also called holding current. The ratio I_{max}/I_{min} has the value [23]:

$$\left|\frac{I_{max}}{I_{min}}\right| = \frac{(1-2LC\omega^2)}{2LC\omega^2}. \tag{20}$$

B. *The Rectifier with Near Sinusoidal Input Currents (RNSIC-2 topology)*

Next, it is presented a rectifier configuration with near sinusoidal input currents, and three capacitors C_1-C_3, which are connected on AC side (Figure 2). The supply voltages of these capacitors are limited to $\pm V_d$.

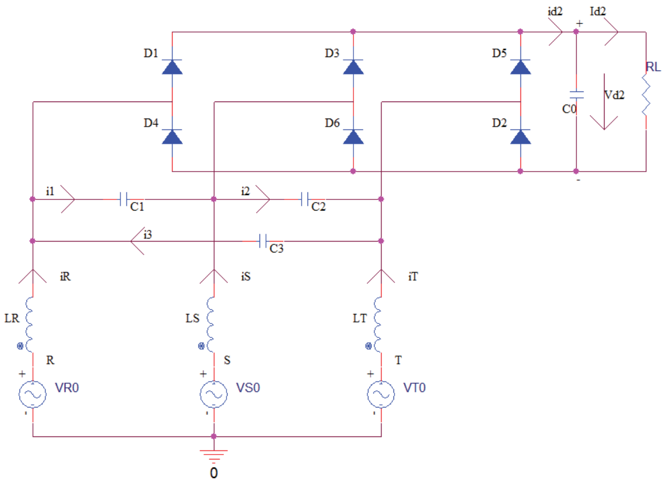

Figure 2. The RNSIC-2 electric scheme [30]

The φ angle variation between the phase voltage and phase current (V_{R0} and i_R) depends on the V_{d2} and V_{dmax} ratio.

For the higher load currents I_{d2}, with $0 \le \omega t \le \pi/3$, for both topologies, RNSIC-1 and RNSIC-2, the phase current waveforms and the conduction period of D_1-D_6 diodes are identical.

A distinction can be observed at the small load currents I_{d2}, with $\pi/3 \le \omega t \le 2\pi/3$, when the diodes conduction periods are different: for the RNSIC-2 topology none or two diodes can be simultaneous in conduction [23].

C. *The Rectifier with Near Sinusoidal Input Currents (RNSIC-3 topology)*

This RNSIC topology is composed of three series inductors L_R, L_S, and L_T and commutation capacitors C_1-C_3 (See Figure 3). For small currents, the RNSIC-3 is considered to be equivalent with RNSIC-1. Although it has a simple configuration, it has the largest DC current ripple [33].

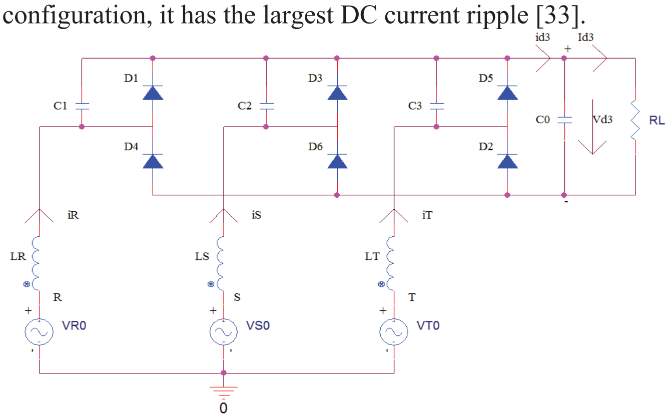

Figure 3. The RNSIC-3 electric scheme [33]

Such an active filter is placed in the network node, and serves multiple loads. This case does not absolutely exclude the appearance of some resonances due to both the presence of some capacitors bank, and the current harmonics. For the small nonlinear loads, it can be used so many RNSIC converters as many loads exist. Therefore, it is avoided the appearance of the current harmonics in different parts of the supply network.

IV. Results and Analysis

This section presents the PQ indices calculation involving the three rectifier topologies with near sinusoidal input currents (RNSIC), and DWT and FFT comparative analysis of these values.

The experimental tests on a lab stand use the filtering capacitor C_0 of 4700 µF, the inductance L_1-L_3 equal with 16 mH, the CS411299 rectifier bridge with D_1-D_6 diodes and the load resistor R_L = 100 Ω. The AC input voltage magnitude V_{m1} is equal to 325 V. The RNSIC converter configuration also contains the C_1-C_6 capacitors (for RNSIC-1) or C_1-C_3 capacitors (for RNSIC-2 and RNSIC-3), with 60 µF value (See Figure 4).

The waveforms of voltage and current are obtained using a data acquisition system with linear/nonlinear loads composed of a Digital Signal Processor (DSP) board with high-speed 12 bit Analog to Digital Converters (ADC), which coupled to three-phase systems using the Hall transducers.

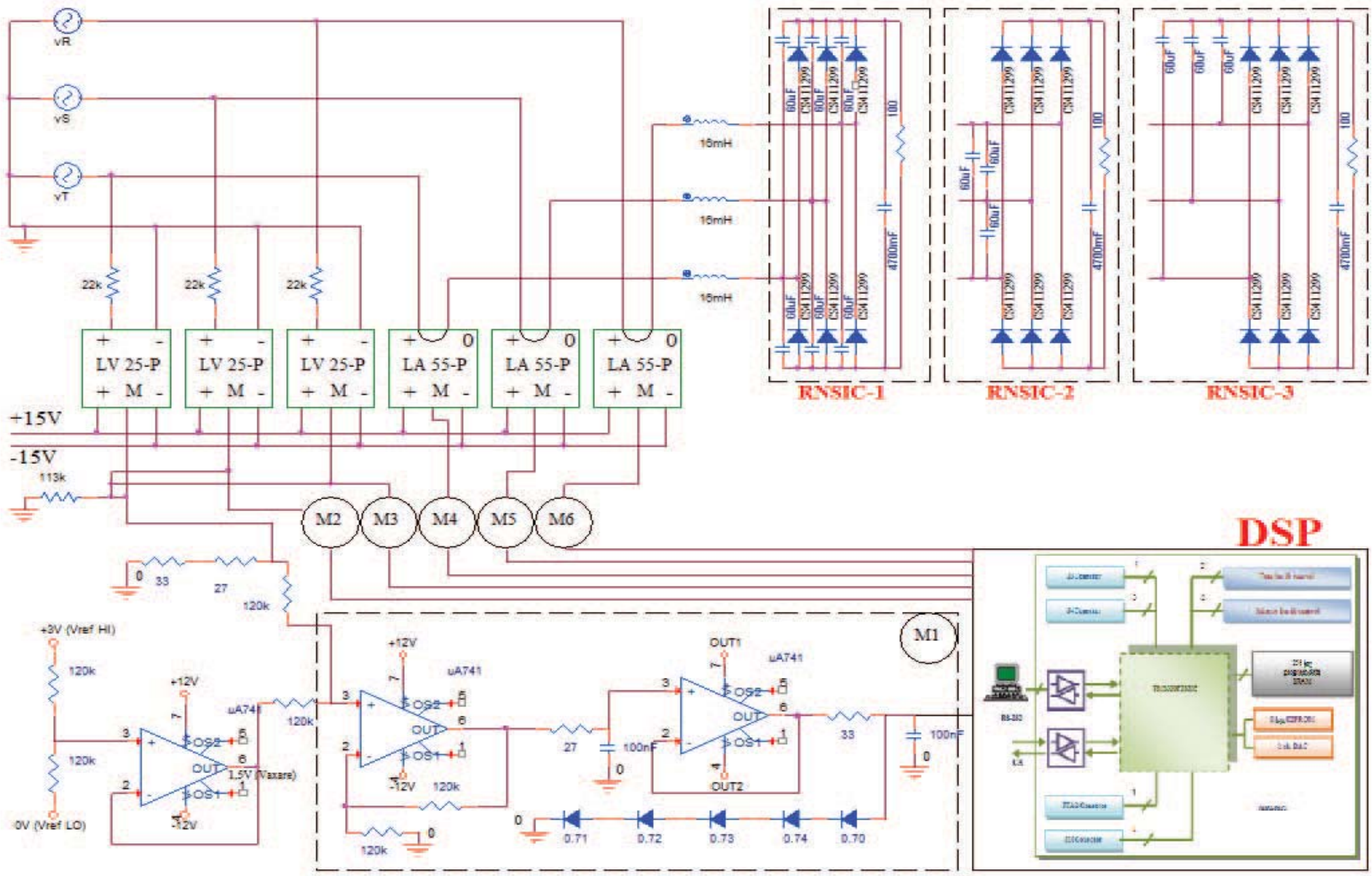

Figure 4. The data acquisition system with Hall transducers with RNSIC

The phase voltage waveforms V_R (CH2, 100 V/div.) and the phase current waveforms I_R (CH1, 10 A/div.) captured using the oscilloscope are shown in Figure 5. For a 50 Hz frequency and 5 ms period it can be seen that the R phase current waveform is sinusoidal. The AC input voltage magnitude V_{m1} is equal to 325 V.

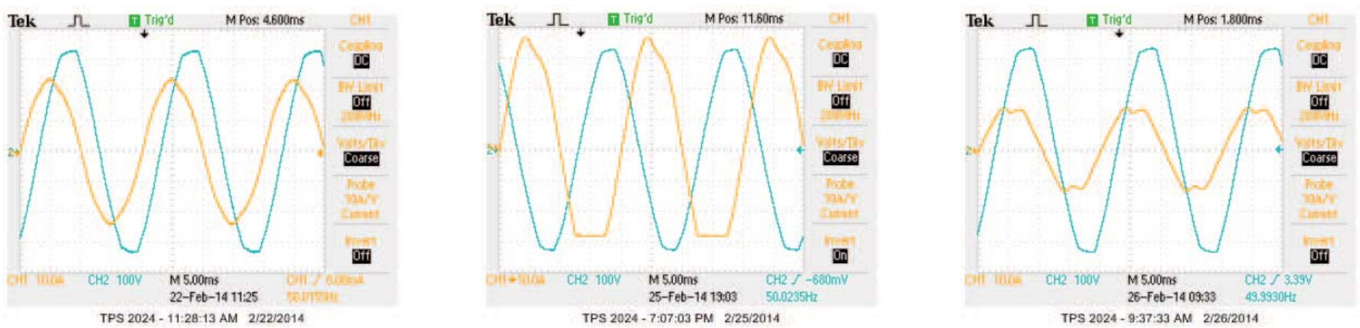

(a) (b) (c)

Figure 5. The current and voltage phase R waveforms of RNSIC with resistive load R_L = 100 Ω: (a) RNSIC-1, (b) RNSIC-2 and (c) RNSIC-3

For RNSIC-1 the current harmonic components represent only 3.83% of the current fundamental harmonic, while for RNSIC-2 and RNSIC-3, it represents 10.6 and 8.15, respectively (see Figure 6).

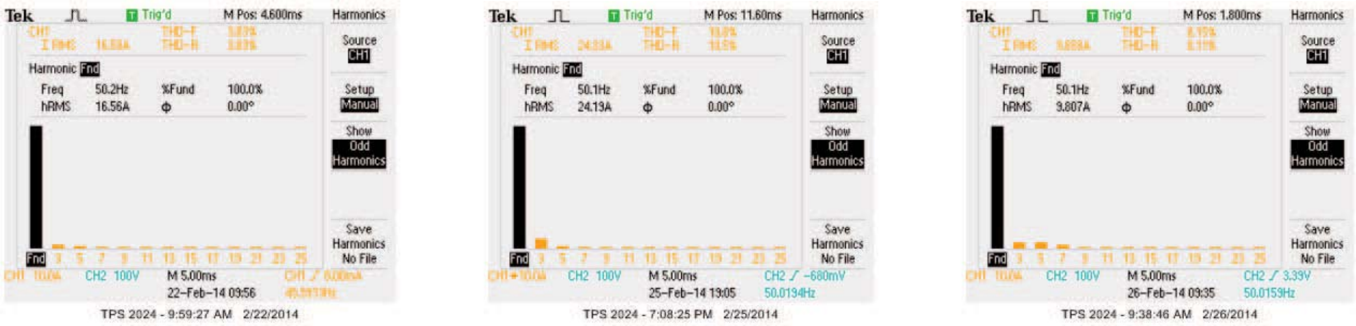

(a) (b) (c)

Figure 6. The spectrum of I_R phase current for RNSIC with resistive load R_L = 100 Ω: (a) RNSIC-1, (b) RNSIC-2 and (c) RNSIC-3

A frequency domain analysis using FFT, and a time-frequency domain analysis using DWT have been carried out by Matlab software. The results are presented in Table I. The power quality indices were calculated for two resistive loads of 100 Ω, and 3.2 kΩ, respectively.

In wavelet analysis, it was used the 'db10' (Daubechies), which is considered the most suitable mother wavelet, due to its capacity of giving the least deviation between the calculated percentage energy of the harmonics and the percentage energy of the coefficients for the wavelet levels [11].

TABLE I. PQIS VALUES FOR RECTIFIER WITH NEAR SINUSOIDAL INPUT CURRENTS SYSTEMS

	PQ index	Electric component	RNSIC-1		RNSIC-2		RNSIC-3	
			FFT approach	*DWT approach*	*FFT approach*	*DWT approach*	*FFT approach*	*DWT approach*
R_L = 100 Ω, V_{m1} = 325 V, f = 50 Hz	**Equivalent Total Harmonic Distortion**	THD_v	0.0183	0.0187	0.2101	0.2136	0.1523	0.1519
		THD_i	0.0144	0.0148	0.1145	0.1158	0.0743	0.0741
	Distortion index	DIN_v	0.0184	0.0192	0.2045	0.2057	0.1411	0.1415
		DIN_i	0.0143	0.0146	0.1094	0.1103	0.0694	0.0703
	Transformer K-factor	K	1.9256	1.9386	3.1454	3.1422	2.6457	2.6430
	Phase crest factor	CF_R	1.72	1.74	1.84	1.84	1.79	1.80
		CF_S	1.74	1.75	1.86	1.87	1.82	1.79
		CF_T	1.73	1.72	1.89	1.88	1.80	1.81
	Overall crest factor	CF	1.74	1.75	1.89	1.88	1.82	1.81
R_L = 3.2 kΩ, V_{m1} = 325 V, f = 50 Hz	**Equivalent Total Harmonic Distortion**	THD_v	0.2078	0.2085	0.2142	0.2139	0.2452	0.2454
		THD_i	0.1124	0.1128	0.1432	0.1437	0.2064	0.2061
	Distortion index	DIN_v	0.2034	0.2036	0.2103	0.2100	0.2447	0.2446
		DIN_i	0.1117	0.1121	0.1388	0.1391	0.2031	0.2033
	Transformer K-factor	K	3.4256	3.5467	3.5678	3.5680	3.7415	3.7411
	Phase crest factor	CF_R	1.79	1.82	1.81	1.83	1.92	1.93
		CF_S	1.92	1.95	1.92	1.91	1.95	1.96
		CF_T	1.87	1.90	1.90	1.91	1.97	1.98
	Overall crest factor	CF	1.92	1.95	1.92	1.91	1.97	1.98

V. CONCLUSION

This paper has proposed a comparative analysis of the power quality indices obtained with DWT and FFT using three rectifier topologies with near sinusoidal input currents.

The experimental results highlight the fact that DWT based definitions are more accurate, and that they can be used successfully for non-stationary voltage and current waveforms.

The values of FFT-based indices are very close to the values of DWT-based indices, which demonstrates the efficiency of the latter method.

Comparing the outcomes corresponding to the three rectifier topologies, it can be seen that for RNSIC-1, the current harmonic components percentage is smaller than the other two (RNSIC-2 and RNSIC-3), which means that the current waveform is sinusoidal.

ACKNOWLEDGMENT

This paper was supported by the project "Improvement of the doctoral studies quality in engineering science for development of the knowledge based society-QDOC" contract no. POSDRU/107/1.5/S/78534, project co-funded by the European Social Fund through the Sectorial Operational Program Human Resources 2007-2013.

REFERENCES

[1] Electromagnetic Compatibility (EMC-Part 4–7: Testing and Measurement Techniques-General Guide on Harmonics and Interharmonics Measurement and Instrumentation, for Power Supply Systems and Equipment Connected Thereto, 2002. IEC 61000-4-7.

[2] IEEE Recommended Practices and Requirements for Harmonics Control in Electrical Power Systems, IEEE Standard 519-1992;

[3] Electromagnetic Compatibility (EMC) Part 4-30: Testing and Measuring Techniques-Power Quality Measurement Methods, IEC 61000-4-30, Jan. 1997.

[4] U. Gudaru and V.B. Waje "Analysis of harmonics in power system using wavelet transform", *IEEE Students' Conference on Electrical, Electronics and Computer Science*, 2012, pp. 1-5.

[5] V. Apetrei, C. Filote and C. Ciufudean, "Effective Value Calculation Using Wavelet Transform", *Recent Researches in Electric Power and Energy Systems, Proceedings of the 13th International Conference on Electric Power Systems, High Voltages, Electric Machines*, vol. 22, Aug. 2013, pp. 204-210.

[6] R. Shariatinasab, M. Akbari and B. Rahman, "Application of Wavelet Analysis in Power Systems", *Advances in Wavelet Theory and Their Applications in Engineering, Physics and Technology*, 2012, pp.221-244.

[7] W.-K. Yoon and M. J. Devaney, "Power measurement based on the wavelet transform", *IEEE Trans. Instrum. Meas.*, vol. 47, Oct. 1998, pp. 1205-1210.

[8] W.-K. Yoon and M. J. Devaney, "Reactive power measurement using the wavelet transform", *IEEE Trans. Instrum. Meas.*, vol. 49, no. 2, Apr. 2000, pp. 246-252.

[9] E. Y. Hamid, Z. Kawasaki and R. Mardiana, "Wavelet packet transform for RMS and power measurements", in *Proc.2001 IEEE Power Engineering Society Summer Meeting*, Jul. 2001, pp. 1243-1245.

[10] S. Mallat, *A Wavelet Tour of Signal Processing*. New York: Academic, 1999.

[11] W.G. Morsi and M. E. El-Hawary "The Most Suitable Mother Wavelet for Steady-State Power System Distorted Waveforms", *Conference on Electrical and Computer Engineering*, 2008, pp. 17-22.

[12] G.S. Kumar, D.V.S. Sarma and C. Venkatesh "Wavelet Transform Based Harmonic Analysis and Real Power Measurement", *International Conference on Power Electronics*, Jan. 2011, pp. 1-6.

[13] W.G. Morsi and M.E. El-Hawary, "Wavelet Packet Transform-Based Power Quality Indices for Balanced and Unbalanced Three-Phase Systems Under Stationary or Nonstationary Operating Conditions", *IEEE Transactions on Power Delivery*, vol. 24, no.4, 2009, pp. 2300-2310.

[14] L.C. Saikia, S.M. Borah and S. Pait, S. "Detection and classification of power quality disturbances using wavelet transform, fuzzy logic and neural network", *Annual IEEE India Conference*, 2010, pp. 1-5.

[15] S. Vanga and S.N.V. Ganesh "Comparison of Fourier Transform and Wavelet Packet Transform for quantification of power quality", *International Conference on Advances in Power Conversion and Energy Technologies*, 2012, pp. 1-6.

[16] Yu Chen "Harmonic Detection in Electric Power System Based on Wavelet Multi-resolution Analysis", *International Conference on Computer Science and Software Engineering*, 2008, pp. 1204- 1207.

[17] H. Albert and L. Elefterescu "Harmonic and Unbalance Disturbances Monitoring", *The 5th International Power Systems Conference*, Nov. 2003, pp. 19-26.

[18] IEEE Trial-Use Standard Definitions for the Measurement of Electric Power Quantities Under Sinusoidal, Non-Sinusoidal, Balanced, or Unbalanced Conditions, June 2000, IEEE Standard 1459.

[19] IEEE Standard Definitions for the Measurement of Electric Quantities Under Sinusoidal, Non-Sinusoidal, Balanced, or Unbalanced Conditions, Mar. 2010, IEEE Standard 1459.

[20] W. G. Morsi and M.E. El-Hawary, "Reformulating Three-Phase Power Components Definitions Contained in the IEEE Standard 1459–2000 Using Discrete Wavelet Transform", *IEEE Transactions on Power Delivery*, vol. 22, no. 3, 2007, pp. 1917-1925.

[21] A. Mansour, Z. Changning and H. Nasry, "Measurement of Power Components in Balanced and Unbalanced Three-Phase Systems Under Nonsinusoidal Operating Conditions by Using IEEE Standard 1459-2010 and Fourier Analysis", *International Conference on Technological Advances in Electrical, Electronics and Computer Engineering*, May 2013, pp. 166-171.

[22] I.-D. Nicolae and P.-M. Nicolae "Using Discrete Wavelet Transform to Evaluate Power Quality at Highly Distorted Three-Phase Systems", *11th International Electrical Power Quality and Utilisation*, Oct. 2011, pp. 1-6.

[23] M. Pletea, N.R. Buzatu, A. Serediuc, C. Nedelcu and I.V. Pletea "Variants of rectifiers with near sinusoidal input currents", *10th International Symposium on Signals, Circuits and Systems*, June 2011, pp. 1-4.

[24] C. Filote, C. Ciufudean and A.M. Cozgarea "An analysis of Rectifiier with Near Sinusoidal input current", *International Conference on Clean Electrical Power*, July 2009, pp. 580 – 584.

[25] D. Alexa, A. Sîrbu, I.V. Pletea and T.C. Goras "Hybrid Rectifier With Near-Sinusoidal Input Currents", *IEEE Transactions on Industrial Electronics*, vol. 59, no. 7, July 2012, pp. 2947 - 2958.

[26] C. Filote, C. Ciufudean and A.M. Cozgarea "A comparative analysis of total harmonic distortion in TPRD and RNSIC", *13th European Conference on Power Electronics and Applications*, Sept. 2009, pp. 1-8.

[27] D. Alexa, T.C. Goras, A. Sarbu, I.V. Pletea, C. Filote, F. Ionescu "Analysis of the two-quadrant converter with rectifier with near sinusoidal input currents", *IET Power Electronics*, vol. 1, no. 2, June 2008, pp. 224 - 234.

[28] C. Filote, C. Ciufudean, S. Alaci and A.M. Cozgarea "Harmonie elimination and power factor improvement of three-phase rectifier using RNSIC variant", *International Conference on Clean Electrical Power (ICCEP)*, June 2011, pp. 40-45.

[29] D. Alexa, T.C. Goras, I.V. Pletea, R. Buzatu, M. Moisa and R. Chiper "Analysis of the two-quadrant converter having rectifier with near sinusoidal input currents and capacitors connected on the AC side", *International Symposium on Signals, Circuits and Systems (ISSCS)*, July 2009, pp: 1-4.

[30] D. Alexa, A. Sarbu, I.V. Pletea, C. Filote and R. Chiper "Variants of rectifiers with near sinusoidal input currents - a comparative analysis with the conventional diode rectifier", *IET - Power Electronics*, July 2011, pp: 632 – 641.

[31] C. Filote, C. Ciufudean, S. Alaci and A.M. Cozgarea "Wavelet multi-resolution analysis of TPRD and RNSIC input current", *11th WSEAS International Conference on signal processing, computational geometry and artificial vision*, Aug. 2011, pp: 158-165.

[32] G. Raţă, M. Raţă, C. Filote, C. Strugaru, "Theoretical and experimental aspects concerning Fourier and wavelet analysis for deforming consumers in power network", *Electronics and Electrical Engineering Journal*, no. 1 (97), 2010, pp. 62-66.

[33] Z. Chen and Y. Luo „Low-Harmonic-Input Three-Phase Rectifier With Passive Auxiliary Circuit: Comparison and Design Consideration", *IEEE Transactions on Industrial Electronics*, vol. 58, no. 6, June 2011, pp. 2265-2273.

[34] X. Wang, F. Blaabjerg, Z. Chen, "Autonomous control of Inverter-Interfaced Distributed Generation Units for Harmonic Current Filtering and Resonance Damping in an Islanded Microgrid", *IEEE Transaction on Industrial Applications,* Vol. 50, No. 1, 2014, pp. 452-461.

[35] C. L. Cooper, R. O. Pragale, T. J. Dionise, "A Systematic Approach for Medium-Voltage Power Factor Correction Design, "*IEEE Transaction on Industrial Applications,* Vol. 49, No. 3, 2013, pp. 1043-1055.